Spectrochimica Acta Part A 84 (2011) 243–248

Contents lists available at SciVerse ScienceDirect

Spectrochimica Acta Part A: Molecular and Biomolecular Spectroscopy

journal homepage: www.elsevier.com/locate/saa

# Effect of substituent of terpyridines on the DNA-interaction of polypyridyl ruthenium(II) complexes

Mohan N. Patel*, Deepen S. Gandhi, Pradhuman A. Parmar

*Department of Chemistry, Sardar Patel University, Vallabh Vidyanagar-388 120, Gujarat, India*

ARTICLE INFO

*Article history:*
Received 28 April 2011
Received in revised form
10 September 2011
Accepted 14 September 2011

*Keywords:*
Mixed ligand ruthenium(II) complex
Substituted terpyridines
DNA-interaction
Ionic strength

ABSTRACT

An octahedral complexes of ruthenium with 2,9-dimethyl-1,10-phenanthroline (dmphen) and substituted terpyridine have been synthesized. The $Ru^{II}$ complexes have been characterized by elemental analyses, thermogravimetric analyses, magnetic moment measurements, FT-IR, electronic, $^1H$ NMR and FAB mass spectra. The binding strength and mode of interaction of the complexes with Herring Sperm DNA has been investigated using absorption titration and viscosity measurement studies. Results suggest that the substituent on terpyridine ligand affects the binding mode and binding ability of the complexes. Effect of time and ionic strength on DNA cleavage ability of complex has also been studied by gel electrophoresis. Results suggest that more than 200 mM concentration of NaCl decreases the cleavage ability of complex.



## 1. Introduction

Metal complexes binding with nucleic acid are currently investigated because of their utility as DNA structural probes, DNA foot printing and specific cleavage agents, and potential anticancer drug [1]. Studies of the interaction of transition metal complexes with DNA have been a pet subject of researchers in the field of bioinorganic chemistry [2]. Transition-metal complexes are well suited for application as artificial nucleases, because of their diverse structural features, and the possibility to tune their redox potential through the choice of proper ligands [3]. Synthetic routes to 2,2′:6′,2″-terpyridines have attracted considerable interest because these heterocycles are used extensively in both coordination chemistry and supramolecular chemistry [4,5].

Dipyridyl complexes of ruthenium have been reported to show high excited state potential but are not very efficient DNA intercalators, while phenanthroline complexes of ruthenium are reported to bind DNA via intercalation. The ruthenium complexes of terpyridine ligands are more rigid compared to bipyridine ligands, and have not been investigated systematically. The complexes of terpyridine moieties have several synthetic and structural advantages over the bipyridine complexes [2]. As far as $Ru^{II}$ complexes with tridentate ligands, the concerned studies have received a limited degree of attention, because interest in such complexes is restricted by the absence of room temperature luminescence of $[Ru(tpy)_2]_2$ [6], and their exact mode and extent of DNA-binding still remain unknown. Therefore, extensive studies on structurally different tridentate ligands are necessary to further evaluate and understand the factors that determine the DNA-binding mode and extent [7]. The octahedral polypyridyl $Ru^{II}$ complexes bind to DNA in three dimensions, but the ancillary ligands can also play an important role in governing DNA-binding of the complexes. By varying substitutive group or substituent position in the ancillary ligand creates some interesting differences in the space configuration and the electron density distribution of $Ru^{II}$ polypyridyl complexes, which will result in some differences in spectral properties and the DNA-binding behaviors of the complexes, and will be helpful to understand the binding mechanism of $Ru^{II}$ polypyridyl complexes to DNA [8].

In this article, we report the synthesis and characterization of three complexes: $[Ru^{II}(4\text{-cptpy})(dmphen)Cl]ClO_4$ (**1**), $[Ru^{II}(ptpy)(dmphen)Cl]ClO_4$ (**2**) and $[Ru^{II}(4\text{-ttpy})(dmphen)Cl]ClO_4$ (**3**), where 4-cptpy = 4′-(4-chlorophenyl)-2,2′:6′,2″-terpyridine, ptpy = 4′-phenyl-2,2′:6′,2″-terpyridine, 4-ttpy = 4′-(4-tolyl)-2,2′:6′,2″-terpyridine, dmphen = 2,9-dimethyl-1,10-phenanthroline. Binding behaviors of the synthesized complexes towards Herring Sperm DNA have been investigated using absorption titration and viscosity measurement methods. Cleavage of pUC19 DNA by the complexes has also been studied by gel electrophoresis technique.

## 2. Experimental

### 2.1. Materials and chemicals

2-Acetyl pyridine, 4-chlorobenzaldehyde, benzaldehyde and 4-methylbenzaldehyde were purchased from Spectrochem

* Corresponding author. Tel.: +91 2692226858x221.
*E-mail address:* jeenen@gmail.com (M.N. Patel).

1386-1425/$ – see front matter © 2011 Elsevier B.V. All rights reserved.
doi:10.1016/j.saa.2011.09.037

(Mumbai, India). Ruthenium trichloride and sodium perchlorate were purchased from Chemport (Mumbai, India). Luria Broth, agarose, ethidium bromide (EB), TAE (Tris–Acetyl–EDTA), bromophenol blue and xylene cyanol FF were purchased from Himedia, India. Herring Sperm DNA was purchased from Sigma Chemical Co., India. 2,9-Dimethyl-1,10-phenanthroline was purchased from Loba Chemie (India). Culture of pUC19 bacteria (MTCC 47) was purchased from Institute of Microbial Technology, Chandigarh, India.

### 2.2. Physical measurements

Infrared spectra were recorded on Fourier transform IR (FTIR) Shimadzu spectrophotometer as KBr pellets in the range 4000–400 $cm^{-1}$. The $^1H$ NMR and $^{13}C$ NMR were recorded on a Bruker Avance (400 MHz). The fast atomic bombardment mass spectra (FAB MS) were recorded on Jeol SX 102/Da-600 mass spectrometer/data system using Argon/Xenon (6 kV, 10 mA) as the FAB gas. The accelerating voltage was 10 kV and spectra were recorded at room temperature. The electronic spectra were recorded on a UV-160A UV–Vis spectrophotometer, Shimadzu (Japan). TGA was carried out using a 5000/2960 SDTA, TA instrument (USA) operating at a heating rate of 10 °C per minute in the range of 20–800 °C under $N_2$. C, H and N elemental analyses were performed with a model 240 Perkin Elmer elemental analyzer. The magnetic moments were measured by Gouy's method using mercury tetrathiocyanatocobaltate(II) as the calibrant ($\chi_g = 16.44 \times 10^{-6}$ cgs units at 20 °C), with a Citizen Balance.

### 2.3. Synthesis of ligands

#### 2.3.1. Synthesis of 4′-(4-chlorophenyl)-2,2′:6′,2″-terpyridine (4-cptpy)

2-Acetylpyridine (2.42 g, 20.0 mmol) was added to 70 mL ethanolic solution of 4-chlorobenzaldehyde (1.4 g, 10.0 mmol). KOH pellets (1.4 g, 26 mmol) and aqueous $NH_3$ (30 mL, 25%, 0.425 mol) were added to the solution and was then stirred at room temperature for 8 h (Scheme 1). An off-white solid was formed which was collected by filtration and washed with $H_2O$ (3× 10 mL) and ethanol (2× 5 mL). Recrystallization from $CHCl_3$–MeOH gave white crystalline solid. Yield: 1.48 g, 43%, mp: 168–169 °C. $^1H$ NMR ($CDCl_3$, 400 MHz) $\delta$/ppm 8.753–8.744 (m, 4H, $H_{3,3',5',3''}$), 8.697 (d, 2H, $H_{6,6''}$), 7.939–7.859 (m, 4H, $H_{4,4''}$, $H_{ph2,6}$), 7.495 (d, 2H, $H_{ph3,5}$), 7.390 (dd, 2H, $H_{5,5''}$). $^{13}C$ NMR ($CDCl_3$, 100 MHz) $\delta$/ppm 156.24 ($C_{2',6'}$), 155.74 ($C_{2,2''}$), 149.24 ($C_{4'}$), 148.81 ($C_{6,6''}$), 137.4 ($C_{4,4''}$), 136.82 ($C_{ph1}$), 135.3 ($C_{ph4}$), 129.23 ($C_{ph2,6}$), 128.65 ($C_{ph3,5}$), 123.96 ($C_{5,5''}$), 121.65 ($C_{3,3''}$), 118.83 ($C_{3',5'}$). Anal. Calc. for $C_{21}H_{14}ClN_3$: C, 73.36; H, 4.10; N, 12.22. Found: C, 73.12; H, 4.24; N, 12.06. UV–Vis (DMSO): λ/nm ($\varepsilon_{max}$/$dm^3$ $mol^{-1}$ $cm^{-1}$) 280.5 ($3.1 \times 10^4$).

#### 2.3.2. Synthesis of 4′-phenyl-2,2′:6′,2″-terpyridine (ptpy)

The ligand was prepared by the same method as described above, but using benzaldehyde (1.06 g, 10 mmol) instead of 4-chlorobenzaldehyde. Yield: 1.11 g, 36%, mp: 202–204 °C. $^1H$ NMR ($CDCl_3$, 400 MHz) $\delta$/ppm 8.802 (s, 2H, $H_{3',5'}$), 8.771 (d, 2H, $H_{3,3''}$), 8.72 (d, 2H, $H_{6,6''}$), 7.959–7.91 (m, 4H, $H_{4,4''}$, $H_{ph2,6}$), 7.556–7.456 (m, 3H, $H_{ph3,4,5}$), 7.395 (dd, 2H, $H_{5,5''}$). $^{13}C$ NMR ($CDCl_3$, 100 MHz) $\delta$/ppm 155.88 ($C_{2',6'}$), 155.55 ($C_{2,2''}$), 150.47 ($C_{4'}$), 148.78 ($C_{6,6''}$), 138.31 ($C_{ph1}$), 137.32 ($C_{4,4''}$), 129.11 ($C_{ph2,6}$), 127.39 ($C_{ph3,4,5}$), 123.94 ($C_{5,5''}$), 121.6 ($C_{3,3''}$), 119.2 ($C_{3',5'}$). Anal. Calc. for $C_{21}H_{15}N_3$: C, 81.53; H, 4.89; N, 13.58. Found: C, 81.32; H, 4.71; N, 13.41. UV–Vis (DMSO): λ/nm ($\varepsilon_{max}$/$dm^3$ $mol^{-1}$ $cm^{-1}$) 279.5 ($3.7 \times 10^4$).

#### 2.3.3. Synthesis of 4′-(4-tolyl)-2,2′:6′,2″-terpyridine (4-ttpy)

The ligand was prepared by the same method as described above but using 4-methylbenzaldehyde (1.2 g, 10 mmol) instead of 4-chlorobenzaldehyde. Yield: 1.26 g, 39%, mp: 151–152 °C. $^1H$ NMR ($CDCl_3$, 400 MHz) $\delta$/ppm 8.798 (s, 2H, $H_{3',5'}$), 8.776 (d, 2H, $H_{3,3''}$), 8.721 (d, 2H, $H_{6,6''}$), 7.924 (dd, 2H, $H_{4,4''}$), 7.869 (d, 2H, $H_{ph2,6}$), 7.404 (dd, 2H, $H_{5,5''}$), 7.344 (d, 2H, $H_{ph3,5}$), 2.453 (s, 3H, $CH_3$). $^{13}C$ NMR ($CDCl_3$, 100 MHz) $\delta$/ppm 156.26 ($C_{2',6'}$), 155.75 ($C_{2,2''}$), 150.18 ($C_{4'}$), 148.98 ($C_{6,6''}$), 139.1 ($C_{ph1}$), 136.92 ($C_{4,4''}$), 135.45 ($C_{ph4}$), 129.66 ($C_{ph3,5}$), 127.15 ($C_{ph2,6}$), 123.75 ($C_{5,5''}$), 121.42 ($C_{3,3''}$), 118.7 ($C_{3',5'}$), 21.25 ($CH_3$). Anal. Calc. for $C_{22}H_{17}N_3$: C, 81.71; H, 5.30; N, 12.99. Found: C, 81.96; H, 5.13; N, 13.12. UV–Vis (DMSO): λ/nm ($\varepsilon_{max}$/$dm^3$ $mol^{-1}$ $cm^{-1}$) 283.0 ($3.5 \times 10^4$).

### 2.4. Synthesis of complexes

#### 2.4.1. Synthesis of [$Ru^{II}$(4-cptpy)(dmphen)Cl]$ClO_4$ (**1**)

The [$Ru^{III}$(4-cptpy)$Cl_3$] (5 mmol) was synthesized by stirring 4-cptpy in ethanol (500 mL) with gentle heating till dissolution followed by addition of $RuCl_3 \cdot 3H_2O$ (5 mmol) to it and the solution was refluxed for 3 h with stirring. The mixture was allowed to cool at room temperature resulting in the formation of brown precipitate. The precipitate was filtered off and was washed with ethanol and ether followed by drying in air [9]. The complex [$Ru^{III}$(4-cptpy)$Cl_3$] (280 mg, 0.5 mmol), 2,9-dimethyl-1,10-phenanthroline (114 mg, 0.55 mmol), excess LiCl (122 mg, 2.94 mmol) and $NEt_3$ (0.9 mL) were taken in 50 mL ethanol and the mixture was refluxed for 2 h under a dinitrogen atmosphere (Scheme 1). In this reaction, $NEt_3$ functions as a reducing agent and facilitates dissociation of the Ru–Cl Bond. The initial dark brown color of the solution gradually changed to a deep purple. The solvent was then removed under reduced pressure. The dry mass was dissolved in a minimum volume of acetonitrile and an excess saturated aqueous solution of $NaClO_4$ was added to it. The precipitate was filtered off and washed with cold ethanol followed by ice-cold water. The product was dried in vacuum and purified using a silica column. The complex was eluted by 2:1 $CH_2Cl_2$/$CH_3CN$. Yield: 0.279 g, 71%, mol. wt. 788.04. IR (KBr): $\nu$ 3066 w,br; 2920 sh; 1603 m,sh; 1498 m,sh; 1088 s,sh; 756 s,sh; 626 vs,sh; 492 w,sh $cm^{-1}$. $^1H$ NMR [dimethyl sulfoxide-$d_6$ (DMSO-$d_6$), 400 MHz] $\delta$/ppm 9.512 (s, 2H, $T_{3',5'}$, where T = Terpyridine), 9.117 (d, 2H, $T_{6,6''}$), 8.491 (d, 1H, $P_7$, where P = Phenanthroline), 8.402 (d, 2H, $T_{3,3''}$), 8.083 (t, 2H, $T_{4,4''}$), 7.875 (d, 2H, $T_{ph3,5}$), 7.864 (s, 2H, $P_{5,6}$), 7.792–7.775 (m, 2H, $P_{4,8}$), 7.757 (d, 1H, $P_3$), 7.557 (d, 2H, $T_{ph2,6}$), 7.295 (t, 2H, $T_{5,5''}$), 3.321 (s, 3H, $CH_3$), 2.747 (s, 3H, $CH_3$). Anal. Calc. for $C_{35}H_{26}Cl_3N_5O_4Ru$: C, 53.34; H, 3.33; N, 8.89%. Found: C, 53.55; H, 3.16; N, 9.05%. FAB MS: $m/z$ = 789 $[M]^+$, 691 $[M–ClO_4+H]^+$, 653 $[M–ClO_4–Cl]^+$, 345 [4-cptpy+2H]$^+$, 209 [dmphen+H]$^+$.

#### 2.4.2. Synthesis of [$Ru^{II}$(ptpy)(dmphen)Cl]$ClO_4$ (**2**)

The complex was synthesized in a manner identical to that described for [$Ru^{II}$(4-cptpy)(dmphen)Cl]$ClO_4$, with [$Ru^{III}$(ptpy)$Cl_3$] (258 mg, 0.5 mmol) in place of [$Ru^{III}$(4-cptpy)$Cl_3$]. Yield: 0.233 g, 62%, mol. wt. 753.6. IR (KBr): $\nu$ 3072 w,br; 2924 sh; 1596 m,sh; 1496 m,sh; 1083 s,sh; 757 s,sh; 623 vs,sh; 496 w,sh $cm^{-1}$. $^1H$ NMR (DMSO-$d_6$, 400 MHz) $\delta$/ppm 9.481 (s, 2H, $T_{3',5'}$), 9.119 (d, 2H, $T_{6,6''}$), 8.44 (d, 2H, $T_{3,3''}$), 8.34 (d, 1H, $P_7$), 8.078 (t, 2H, $T_{4,4''}$), 7.864 (s, 2H, $P_{5,6}$), 7.798–7.778 (m, 2H, $P_{4,8}$), 7.698 (d, 1H, $P_3$), 7.619 (d, 2H, $T_{ph2,6}$), 7.584–7.571 (m, 3H, $T_{ph3,4,5}$), 7.298 (t, 2H, $T_{5,5''}$), 3.354 (s, 3H, $CH_3$), 2.77 (s, 3H, $CH_3$). Anal. Calc. for $C_{35}H_{27}Cl_2N_5O_4Ru$: C, 55.78; H, 3.61; N, 9.29%. Found: C, 55.93; H, 3.49; N, 9.42%. FAB MS: $m/z$ = 753 $[M]^+$, 655 $[M–ClO_4+H]^+$, 619 $[M–ClO_4–Cl]^+$, 311 [ptpy+2H]$^+$, 209 [dmphen+H]$^+$.

#### 2.4.3. Synthesis of [$Ru^{II}$(4-ttpy)(dmphen)Cl]$ClO_4$ (**3**)

The complex was synthesized in a manner identical to that described for [$Ru^{II}$(4-cptpy)(dmphen)Cl]$ClO_4$, with [$Ru^{III}$(4-ttpy)$Cl_3$] (265 mg, 0.5 mmol) in place of [$Ru^{III}$(4-cptpy)$Cl_3$]. Yield: 0.284 g, 74%, mol. wt. 767.62. IR (KBr): $\nu$ 3071 w,br; 2925 sh; 1594

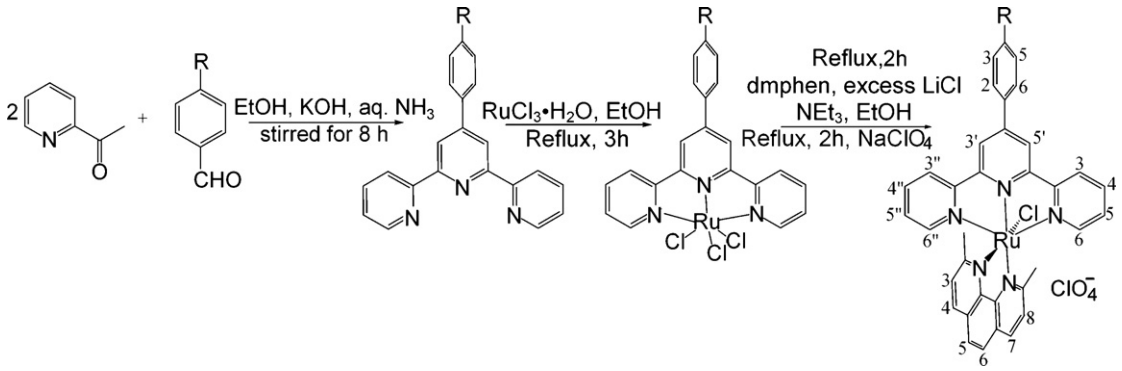


**Scheme 1.** Synthesis of terpyridine ligands and ruthenium(II) complexes (**1**, R=Cl; **2**, R=H; **3**, R=$CH_3$).

m,sh; 1495 m,sh; 1087 s,sh; 762 s,sh; 628 vs,sh; 487 w,sh $cm^{-1}$. $^1H$ NMR (DMSO-$d_6$, 400 MHz) $\delta$/ppm 9.473 (s, 2H, $T_{3',5'}$ 9.124 (d, 2H, $T_{6,6''}$), 8.387 (d, 2H, $T_{3,3''}$), 8.353 (d, 1H, $P_7$), 8.068 (t, 2H, $T_{4,4''}$), 7.873 (s, 2H, $P_{5,6}$), 7.795–7.773 (m, 2H, $P_{4,8}$), 7.705 (d, 1H, $P_3$), 7.584–7.594 (d, 2H, $T_{ph3,5}$), 7.554 (d, 2H, $T_{ph2,6}$), 7.284 (t, 2H, $T_{5,5''}$), 3.387 (s, 3H, $CH_3$), 2.747 (s, 3H, $CH_3$), 2.525 (s, 3H, $CH_3$). Anal. Calc. for $C_{36}H_{29}Cl_2N_5O_4Ru$: C, 56.33; H, 3.81; N, 9.12%. Found: C, 56.51; H, 3.67; N, 9.26%. FAB MS: $m/z$ = 767 $[M]^+$, 669 $[M-ClO_4+H]^+$, 633 $[M-ClO_4-Cl]^+$, 325 [ptpy+2H]$^+$, 209 [dmphen+H]$^+$.

*Caution*: Perchlorate salts of metal complexes with organic ligands are potentially explosive. Only small amounts of material should be prepared, and these should be handled with care [8,10–12].

### 2.5. Evaluation of binding constants

Influence of DNA on MLCT band of $Ru^{II}$ complexes were measured via UV–Vis absorbance spectra [13–16]. The absorption titration was carried out by keeping the concentration of complex constant (20 μM) and varying the concentration of DNA. The change in absorbance at MLCT band was recorded after each addition of DNA. The intrinsic binding constant $K_b$ was determined according to the following equation [17]:

$$\frac{[DNA]}{\varepsilon_a - \varepsilon_f} = \frac{[DNA]}{\varepsilon_b - \varepsilon_f} + \frac{1}{K_b(\varepsilon_b - \varepsilon_f)}$$

where [DNA] is the concentration of DNA in base pairs, the apparent absorption coefficient $\varepsilon_a$, $\varepsilon_f$ and $\varepsilon_b$ correspond to $A_{obs.}/[Ru]$, the extinction coefficient for the free ruthenium complex for each addition of DNA and the extinction coefficient for the ruthenium complex in the fully bound form, respectively. In plots $[DNA]/(\varepsilon_a-\varepsilon_f)$ *versus* [DNA], $K_b$ is given by the ratio of slope to the y intercept.

### 2.6. Viscosity measurement

Cannon–Ubbelohde viscometer maintained at a constant temperature of 27.0 (±0.1) °C in a thermostatic jacket was used to measure the relative viscosity of DNA solutions in the presence of ethidium bromide or $Ru^{II}$ complexes. The concentrations of the $Ru^{II}$ complex and Herring Sperm DNA were chosen to minimize the volume of $Ru^{II}$ complex added to a solution of DNA. DNA concentration was chosen enough to make changes in the slope maximally distinguishable. A 3.0 mM stock solution of each $Ru^{II}$ complex was prepared. A 0.40 mM solution of Herring Sperm DNA was titrated with the $Ru^{II}$ complex. The $Ru^{II}$ complex to DNA concentration ratio was maintained in the range of 0–0.16. Flow time was measured with a digital stopwatch with an accuracy of 0.01 s. The flow time of each sample was measured three times and an average flow time was calculated. Data were represented graphically as $(\eta/\eta_0)^{1/3}$ *versus* concentration ratio ([Complex]/[DNA]) [18], where $\eta$ is viscosity of DNA in the presence of complex and $\eta_0$ is viscosity of DNA alone. Viscosity values were calculated from the observed flow time of DNA-containing solutions ($t > 100$ s) corrected for the flow time of buffer alone ($t_0$), $\eta = t - t_0$.

### 2.7. Gel electrophoresis

Cleavage of pUC19 DNA (100 μg/mL) by $Ru^{II}$ complexes (200 μM) was measured by the conversion of supercoiled pUC19 DNA to open circular and linear. Gel electrophoresis of pUC19 DNA was carried out in TAE buffer (0.04 M Tris–Acetate, pH 8, 0.001 M EDTA). 15 μL of reaction mixture contains 100 μg/mL plasmid DNA, and complex. To study the effect of ionic strength, reaction mixture contains plasmid DNA, complex and different concentration of NaCl. Reaction mixture was incubated at 37 °C. All reactions were quenched by addition of 3 μL loading buffer (0.25% bromophenol blue, 40% sucrose, 0.25% xylene cyanole, and 200 mM EDTA). The aliquots were loaded directly on to 1% agarose gel and electrophoresed at 50 V in 1X TAE buffer. Gel was stained with 0.5 μg/mL of EB, and was photographed on a UV illuminator. After electrophoresis, the proportion of DNA in each fraction was estimated quantitatively from the intensity of the bands using AlphaDigiDoc™ RT. Version V.4.0.0 PC-Image software.

## 3. Result and discussion

### 3.1. Thermogravimetric analysis and magnetic moment measurement

TGA data of the complexes show no weight loss between the temperature of 80 and 180 °C. So, there is an absence of coordinated or lattice water molecules. Both the ligands decomposed in single step between the temperature ranges 360–600 °C. Magnetic moment value of all complexes is found to be zero, which suggests low-spin configuration with $d^2sp^3$ hybridization for octahedral $Ru^{II}$ complexes.

### 3.2. Electronic absorption analysis

The electronic spectra of ligands show only one band at ~280 nm. The electronic spectra of complexes consist of three well-defined bands in the range 250–500 nm, similar to that observed for [Ru(dpphen)(terpy)Cl]$PF_6$ complex reported by Yoshikawa et al. [19]. The band maxima and molar extinction coefficient of complexes are listed in Table 1. The metal–ligand charge transfer

**Table 1**
Electronic spectral data for the ruthenium(II) complexes.

| Complexes | $\lambda_{max}$/nm ($\varepsilon$/dm$^3$ mol$^{-1}$ cm$^{-1}$) | |
|---|---|---|
| | $\pi \rightarrow \pi^*$ | MLCT |
| **1** | 281.0 (70,150), 311.0 (67,100) | 487.5 (27,100) |
| **2** | 276.0 (61,900), 310.0 (42,100) | 488.5 (17,000) |
| **3** | 284.0 (43,100), 308.0 (44,850) | 490.0 (17,600) |

(MLCT) bands appear at 487.5, 488.5 and 490 nm for complexes **1**, **2** and **3**, respectively. Change in the substitution on terpyridine from electron withdrawing group (–Cl) to electron donating group ($-CH_3$), red shift in the MLCT band is observed. The two higher energy absorption bands were observed from 276 to 284 nm and 308 to 311 nm. These bands are attributed to the ligand centered transitions dmphen($\pi$)→dmphen($\pi^*$) and terpy($\pi$)→terpy($\pi^*$), respectively [19].

### 3.3. Infrared spectroscopy

Infrared spectroscopy of the ligands showed bands at ~1580 cm$^{-1}$ and ~1420 cm$^{-1}$ corresponding to C=C and C=N ring stretching. The band appeared at ~720 cm$^{-1}$ is due to C–H out of plane banding. An additional band appeared at 2934 cm$^{-1}$ in 4-ttpy is due to the C–H stretching of methyl. The presence of perchlorate as a counter ion is confirmed by the very strong, broad band at ~1085 cm$^{-1}$ and the strong, sharp band at around 625 cm$^{-1}$ [20]. A weak, broad band around 3070 cm$^{-1}$ appeared due to aromatic C–H stretching. A sharp band around 2922 cm$^{-1}$ appeared due to C–H stretching of methyl. A sharp band with medium intensity appeared around 1600 and 1497 cm$^{-1}$, characteristic of aromatic ring stretching. An intense, sharp band appeared at ~760 cm$^{-1}$ is a characteristic of ring deformations and C–H out-of-plane deformations. A weak, sharp band was around 487–496 cm$^{-1}$, characteristic of Ru–N stretching mode. A Ru–Cl stretching mode would be expected in the region less than 400 cm$^{-1}$ [21].

### 3.4. $^1H$ NMR

The ligands and complexes display resolvable $^1$H NMR spectra in $CDCl_3$ and DMSO-$d_6$. On coordination to ruthenium ion, chemical shift of the $T_{3',5'}$ and $T_{6,6''}$ show large downfield due to metal-to-ligand $\pi$-back donation [10]. $T_{ph2,6}$ and $T_{ph3,5}$ of complex **1** shows downfield shift, while that of complexes **2** and **3** show upfield shift. One methyl group of dmphen appears in downfield than other due to the diamagnetic anisotropic effect exerted by terpyridine.

### 3.5. Evaluation of binding constants

Electronic absorption titration is employed to study the binding of polypyridyl Ru$^{II}$ complexes with DNA. Complex bind to DNA through intercalation usually results in hypochromism (decrease in absorbance) and bathochromism (red shift), because intercalative mode involves a strong stacking interaction between aromatic chromophore and the base pairs of DNA [13]. Electrostatic interaction of complex with DNA shows lower hypochromicity with no bathochromic shift [10,22]. Complex binds to DNA through partial intercalation, generally resulting in hypochromism and small red shift in absorption titration [17,23–25]. The extent of the hypochromism commonly parallels the intercalative binding strength.

The absorption spectra of [Ru$^{II}$(4-cptpy)(dmphen)Cl]$^+$, [Ru$^{II}$(ptpy)(dmphen)Cl]$^+$ and [Ru$^{II}$(4-ttpy)(dmphen)Cl]$^+$ with increasing concentration of Herring Sperm DNA are shown in Fig. 1. As the concentration of DNA is increased, hypochromism in the MLCT band of each complex is observed (Table 2). A decrease

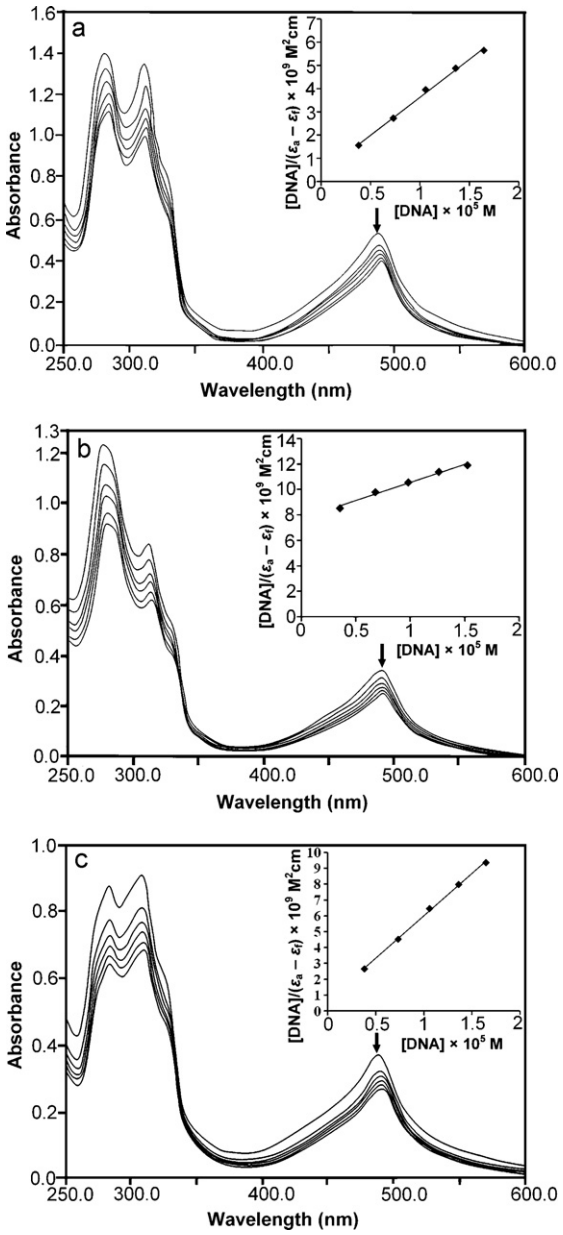


**Fig. 1.** Electronic absorption spectra of (a) [Ru$^{II}$(4-cptpy)(dmphen)Cl]$ClO_4$, (b) [Ru$^{II}$(ptpy)(dmphen)Cl]$ClO_4$ and (c) [Ru$^{II}$(4-ttpy)(dmphen)Cl]$ClO_4$ with increasing amount of DNA in phosphate buffer ($Na_2HPO_4/NaH_2PO_4$, pH 7.2). [Complex] = 20 μM, [DNA] = 0–16.7 μM with incubation period of 15 min at 37 °C. Plots of [DNA]/($\varepsilon_a - \varepsilon_f$) *versus* [DNA] for the titration of DNA with Ru$^{II}$ complexes.

of 19.2% in the MLCT transition is observed for complex **1** with red shift from 487.5 to 490.5 nm ($\Delta\lambda$ = 3 nm). The hypochromism of 4.7 and 17.6% with red shift of 0 and 1 nm is observed for complexes **2** and **3**, respectively. The hypochromism of complex **2** is much smaller than complexes **1** and **3**. Also, complex **2** exhibit

**Table 2**
Electronic absorption data upon addition of Herring Sperm DNA.

| Complex | $\lambda_{max}$ (nm) | | | Hypochromism, $H^a$ (%) | Binding constant, $K_b$ ($M^{-1}$) |
|---|---|---|---|---|---|
| | Free | Bound | $\Delta\lambda$ | | |
| **1** | 487.5 | 490.5 | 3 | 19.2 | $9.21 \times 10^4$ |
| **2** | 488.5 | 488.5 | 0 | 4.7 | $3.71 \times 10^3$ |
| **3** | 490.0 | 491.0 | 1 | 17.6 | $7.88 \times 10^4$ |

[a] $H\% = 100 \times (A_{free} - A_{bound})/A_{free}$.

no red shift for MLCT band. These results suggest that the complex **2** interact with DNA through electrostatic interaction, while complexes **1** and **3** may bind to DNA via classical intercalation or partial intercalation. More confirmation regarding the binding mode of the complexes will be obtained from viscosity measurement.

In order to compare quantitatively the DNA-binding affinities of the three complexes, the intrinsic binding constants ($K_b$) of the complexes with Herring Sperm DNA were determined. From the decay of MLCT band absorbance, the $K_b$ values obtained for complexes **1**–**3** are $9.21 \times 10^4$, $3.71 \times 10^3$ and $7.88 \times 10^4\ M^{-1}$, respectively. These values are comparable to that observed for $[Ru(dmp)_2(ipbp)]^{+2}$ ($7.58 \times 10^3\ M^{-1}$), $[Ru(dmb)_2(ipbp)]^{+2}$ ($1.18 \times 10^4\ M^{-1}$) [11] and $[Ru(tpy)(pta)]$ ($9.51 \times 10^4\ M^{-1}$), [17] but smaller than those observed for $[Ru(bpy)_2(paip)]^{+2}$ ($3.12 \times 10^5\ M^{-1}$) [1] and $[Ru(phen)_2PMIP]^{2+}$ ($8.53 \times 10^5\ M^{-1}$) [26].

Non-planarity of terpyridines, and methyl substitution on phenanthroline ligand, are the main reasons for the lower $K_b$ values. An absence of planarity of the phenyl ring with the basic terpyridine unit affects the magnitude of binding [27]. Substitution on the 2- and 9-positions of the phenanthroline ligand may cause severe steric constraints near the $Ru^{II}$ core when the complex intercalates into the DNA base pairs. The methyl groups may come into close proximity of base pairs at the intercalation sites [11]. Among the complexes, complex **2** shows the least binding strength to double helical DNA, may be due to its electrostatic binding mode. The difference between the $K_b$ values of complexes **1** and **3** is owing to different substituents. The electron-withdrawing substituent (–Cl in 4-cptpy) on the intercalative ligand increases the DNA binding affinity, whereas the electron-releasing substituent ($-CH_3$ in 4-ttpy) decreases the DNA affinity [28].

### 3.6. Viscosity measurement

Viscosity measurement study was carried out to confirm the binding mode of complexes. In classical intercalation, the base pairs are separated to accommodate the binding ligand results in lengthening of the DNA helix and thereby increase the DNA viscosity. A partial and/or non-classical intercalation of compound may bend DNA helix, resulting in the decrease of its effective length and, thereby its viscosity [29]. Electrostatic interaction of compound with DNA does not affect relative viscosity of DNA [30]. The effect of increasing amount of EB and complexes on the relative viscosity of DNA is shown in Fig. 2. EB is a well-known classical intercalator, which increases the relative viscosity of DNA solution. Complex $[Ru(bpy)_3]^{2+}$ has been known to bind with DNA in electrostatic mode, it exerts essentially no effect on DNA viscosity [28]. Complexes **1** and **3** decrease the relative viscosity of DNA as shown by the partial intercalators. No change in relative viscosity is observed for complex **2**, and leads to conclude that complex **2** interacts with DNA via electrostatic interaction. Absorption titration also supports the same binding mode for complex **2** (0 nm red shift). Considering the results of spectroscopic and viscosity measurements, we may suggest that complex **2** shows lowest affinity towards DNA and interacts electrostatically with DNA, while complexes **1** and **3** partially intercalate to DNA.

### 3.7. Effects of time and ionic strength on DNA cleavage

DNA cleavage efficiency of complexes can be achieved by formation of the naturally occurring supercoiled (SC) form to open circular relaxed (OC) form. OC form produced when one of the strands of the plasmid is nicked, and determined by gel electrophoresis of the plasmid. If both strands of the plasmid are nicked, linear (L) form will be generated [31]. SC form migrates faster, OC form migrates slowly while L form migrates in between the SC form and the OC form [32]. Hence, DNA cleavage ability of complexes was

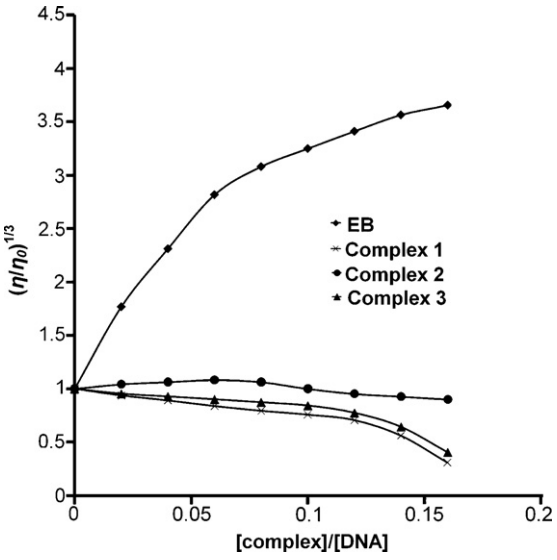


**Fig. 2.** Effect on relative viscosity of DNA under the influence of increasing amount of ethidium bromide (EB) and complexes at $27 \pm 0.1$ °C in phosphate buffer ($Na_2HPO_4/NaH_2PO_4$, pH 7.2).

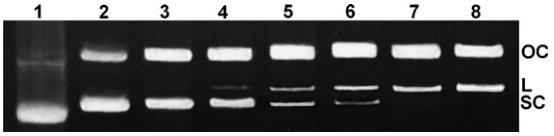


**Fig. 3.** Agarose gel (1%) of pUC19 (100 μg/mL) at 37 °C in TE buffer (pH 8) with 200 μM $[Ru^{II}(4\text{-cptpy})(dmphen)Cl]ClO_4$ complex for increasing incubation time. *Lane 1*, DNA control and *lanes 2–8*, 30, 60, 90, 150, 210, 270 and 360 min, respectively.

quantified by measuring the transformation of the SC form into OC and linear forms.

The time dependence of the reaction was determined in the presence and the absence of the complex. The pUC19 DNA (100 μg/mL) was incubated with 200 μM complex **1** in TE buffer at 37 °C for 30–360 min. The increase in the amount of OC and L forms of DNA was observed to be associated with the increase of reaction time (Fig. 3). The amount of linear DNA was 33% when the reaction time was 360 min. Fig. 4 shows the extent of DNA cleavage by the complex **1** with reaction time. The decrease in the amount of SC form and the formation of OC form of DNA with time shows

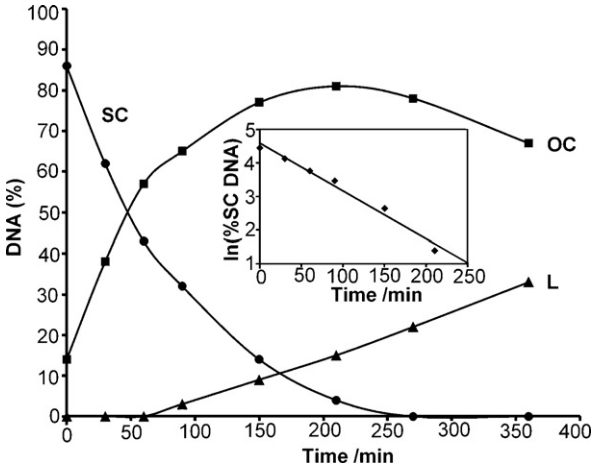


**Fig. 4.** Decrease in the SC form and formation of the OC and L form of pUC19 DNA in the presence of the $[Ru^{II}(4\text{-cptpy})(dmphen)Cl]ClO_4$ complex (200 μM) with incubation time. Inset: ln(% supercoiled form) *versus* time.

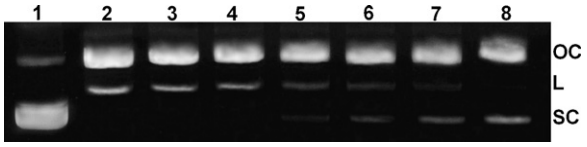


**Fig. 5.** Agarose gel (1%) of pUC19 DNA (100 μg/mL) incubated for 270 min at 37 °C in TE buffer (pH 8) with 200 μM [$Ru^{II}$(4-cptpy)(dmphen)Cl]$ClO_4$ complex for increasing NaCl concentrations. *Lane 1*, DNA control and *lanes 2–8*, NaCl concentration was 25, 50, 100, 200, 400, 600 and 800 mM, respectively.

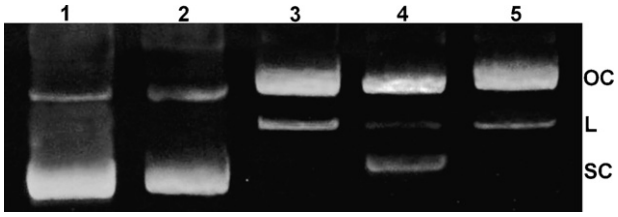


**Fig. 6.** Agarose gel (1%) of pUC19 (100 μg/mL) at 37 °C in TE buffer (pH 8) with 200 μM compounds incubated for 270 min. *Lane 1*, DNA control; *lanes 2*, $RuCl_3$; *lane 3*, [$Ru^{II}$(4-cptpy)(dmphen)Cl]$ClO_4$; *lane 4*, [$Ru^{II}$(ptpy)(dmphen)Cl]$ClO_4$ and *lane 5*, [$Ru^{II}$(4-ttpy)(dmphen)Cl]$ClO_4$.

the exponential nature of the curves. The plot of ln(%SC DNA) *versus* time is linear, which confirms the process is pseudo-first-order. The rate constant $k_1$ ($2.38 \times 10^{-4}\ s^{-1}$), the slope of the linear plot, was obtained using a complex concentration of 200 μM (Fig. 4, inset).

The effects of ionic strength on the double-strand DNA cleavage by adding NaCl were studied. Fig. 5 shows that the process of cleavage was sensitive to the change of ionic strength. The ionic strength could promote DNA cleavage if the concentration of NaCl was less than 200 mM. The amount of the linear form decreased when the ionic strength changed from 200 to 800 mM. Higher concentration of NaCl could make the conformation of DNA tighter, which leads to decrease in DNA cleavage ability of the complex [32]. Fig. 6 shows the cleavage of pUC19 DNA (100 μg/mL) by 200 μM of three complexes after 270 min incubation time. The data show that cleavage efficiency of complex **1** is the highest, while complex **2** has the lowest cleavage efficiency.

## 4. Conclusions

From the results, we conclude that complex with electron withdrawing group shows higher DNA binding affinity than complex with electron donating group. Complexes **1** and **3** bind to DNA via partial intercalation; while complex **2** interacts with DNA through electrostatic interaction. So, the absence of any group on the terpyridine ligand of complex **2** changes the binding mode. The process of decrease in the amount of SC form and the formation of OC form of DNA with time is pseudo-first-order. Concentration of NaCl higher than 200 mM decreases the DNA cleavage ability of complex. Complex **1** cleaves the DNA more efficient than other complexes.

## Conflicts of interest

The authors report no conflicts of interest. The authors alone are responsible for the content and writing of the paper.

## Acknowledgments

Authors thank Head, Department of Chemistry, and Dr. Thakkar, BRD School of Bioscience, Sardar Patel University, India for making it convenient to work in laboratory and UGC for providing financial support under "UGC Research Fellowship in Science for Meritorious Students" scheme.

## References

[1] Y.-J. Liu, C.-H. Zeng, H.-L. Huang, L.-X. He, F.-H. Wu, Eur. J. Med. Chem. 45 (2010) 564–571.
[2] G. Sathyaraj, T. Weyhermüller, B.U. Nair, Eur. J. Med. Chem. 45 (2010) 284–291.
[3] P.U. Maheswari, K. Lappalainen, M. Sfregola, S. Barends, P. Gamez, U. Turpeinen, I. Mutikainen, G.P.V. Wezel, J. Reedijk, Dalton Trans. (2007) 3676–3683.
[4] A. Gehre, S.P. Stanforth, B. Tarbit, Tetrahedron 65 (2009) 1115–1118.
[5] J.C. Adrian, L. Hassib, N.D. Kimpe, M. Keppens, Tetrahedron 54 (1998) 2365–2370.
[6] J.P. Sauvage, J.P. Collin, J.C. Chambron, S. Gillerez, C. Coudret, V. Balzani, F. Barigelletti, L.D. Cola, L. Flamigni, Chem. Rev. 94 (1994) 993–1019.
[7] Y.-J. Liu, J.-C. Chen, F.-H. Wu, K.-C. Zheng, Transition Met. Chem. 34 (2009) 297–305.
[8] L.-F. Tan, H. Chao, Inorg. Chim. Acta 360 (2007) 2016–2022.
[9] P.A. Adcock, F. Richard Keene, R.S. Smythe, M.R. Snow, Inorg. Chem. 23 (1984) 2336–2343.
[10] C.W. Jiang, H. Chao, H. Li, L.-N. Ji, J. Inorg. Biochem. 93 (2003) 247–255.
[11] Y.-J. Liu, X.-Y. Guan, X.-Y. Wei, L.-X. He, W.-J. Mei, J.-H. Yao, Transition Met. Chem. 33 (2008) 289–294.
[12] V. Rajendiran, M. Murali, E. Suresh, M. Palaniandavar, V.S. Periasamy, M.A. Akbarsha, Dalton Trans. (2008) 2157–2170.
[13] H. Deng, J. Li, K.C. Zheng, Y. Yang, H. Chao, L.N. Ji, Inorg. Chim. Acta 358 (2005) 3430–3440.
[14] S. Mudasir, N. Yoshioka, H. Inoue, J. Inorg. Biochem. 77 (1999) 239–247.
[15] L. Fin, P. Yang, J. Inorg. Biochem. 68 (1997) 79–83.
[16] Q.-L. Zhang, J.-G. Liu, H. Chao, G.-Q. Xue, L.-N. Ji, J. Inorg. Biochem. 83 (2001) 49–55.
[17] H. Chao, W.-J. Mei, Q.-W. Huang, L.-N. Ji, J. Inorg. Biochem. 92 (2002) 165–170.
[18] Y.-B. Zeng, N. Yang, W.-S. Liu, N. Tang, J. Inorg. Biochem. 97 (2003) 258–264.
[19] N. Yoshikawa, S. Yamabe, N. Kanehisa, Y. Kai, H. Takashima, K. Tsukahara, Inorg. Chim. Acta 359 (2006) 4585–4593.
[20] C. Eva, A.G.C. Hotze, D.M. Tooke, A.L. Spek, J. Reedijk, Inorg. Chim. Acta 359 (2006) 830–838.
[21] S. Goswami, A.R. Chakravarty, A. Chakravorty, Inorg. Chem. 21 (1982) 2737–2742.
[22] G. Yang, J.Z. Wu, L. Wang, L.-N. Ji, X. Tian, J. Inorg. Biochem. 66 (1997) 141–144.
[23] J. Liu, T.-B. Lu, H. Li, Q.-L. Zhang, L.-N. Ji, Transition Met. Chem. 27 (2002) 686–690.
[24] J.-G. Liu, B.-H. Ye, Q.-L. Zhang, X.-H. Zou, Q.-X. Zhen, X. Tian, L.-N. Ji, J. Biol. Inorg. Chem. 5 (2000) 119–128.
[25] X.L. Wang, H. Chao, X.L. Hong, Y.J. Liu, L.N. Ji, Transition Met. Chem. 30 (2005) 305–311.
[26] H. Xu, Y. Liang, P. Zhang, F. Du, B.-R. Zhou, J. Wu, J.-H. Liu, Z.-G. Liu, L.-N. Ji, J. Biol. Inorg. Chem. 10 (2005) 529–538.
[27] R. Indumathy, M. Kanthimathi, T. Weyhermuller, B.U. Nair, Polyhedron 27 (2008) 3443–3450.
[28] Y.-J. Liu, X.-Y. Wei, W.-J. Mei, L.-X. He, Transition Met. Chem. 32 (2007) 762–768.
[29] J.-G. Liu, Q.-L. Zhang, L.-N. Ji, Y.-Y. Cao, X.-F. Shi, Transition Met. Chem. 26 (2001) 733–738.
[30] M. Chauhan, F.J. Arjmand, Organomet. Chem. 692 (2007) 5156–5164.
[31] V.G. Vaidyanathan, B.U. Nair, J. Inorg. Biochem. 91 (2002) 405–412.
[32] J. Tan, B. Wang, L. Zhu, J. Biol. Inorg. Chem. 14 (2009) 727–739.